MEMS Gyroscopes with Structurally Decoupled 2-DOF Drive and Sense Mode Oscillators

Cenk Acar* and Andrei Shkel**

Microsystems Laboratory, Department of Mechanical and Aerospace Engineering
University of California, Irvine, CA, USA
*cacar@uci.edu, **ashkel@uci.edu, http://mems.eng.uci.edu

ABSTRACT

This paper reports a novel 4 degree-of-freedom non-resonant micromachined gyroscope design concept that addresses two major MEMS gyroscope design challenges: the mode-matching requirement, and instability and drift due to mechanical coupling between the drive and sense modes. The proposed approach is based on utilizing dynamical amplification both in the 2-DOF drive-direction oscillator and the 2-DOF sense-direction oscillator, which are operated in the flat regions of their response curves, to achieve large oscillation amplitudes without resonance. By structurally decoupling the drive and sense modes, operation instability and zero-rate drift is suppressed. Consequently, by utilizing dynamical amplification in the decoupled 2-DOF oscillators, increased bandwidth and reduced sensitivity to structural and thermal parameter fluctuations and damping changes are achieved, leading to improved robustness and long-term stability.

Keywords: Inertial MEMS, micromachined gyroscopes, rate sensors, disturbance rejection, decoupled modes.

1 INTRODUCTION

Micromachined gyroscopes are projected to become a potential alternative to expensive and bulky conventional inertial sensors in a near future. With micromachining processes allowing mass-production of micromechanical systems on a chip together with their control and signal conditioning electronics, low-cost and micro-sized gyroscopes will provide high accuracy rotation measurements leading to an even broader application spectrum, ranging from advanced automotive safety systems and on-chip navigation systems to consumer electronics [1]. However, due to unfavorable effects of scaling, the current state of the art micromachined gyroscopes require an order of magnitude improvement in performance, stability, and robustness [3].

The conventional micromachined rate gyroscopes operate on the vibratory principle of a 2-DOF system with a single proof mass suspended by flexures anchored to the substrate, which render the mass free to oscillate in two orthogonal directions, namely the drive and the sense directions. The overall dynamical system is simply a two degree-of-freedom (2-DOF) mass-spring-damper system, where the drive mode is excited by the electrostatic drive forces, and the sense mode is excited by the rotation-induced Coriolis force, leading to the equations of motion:

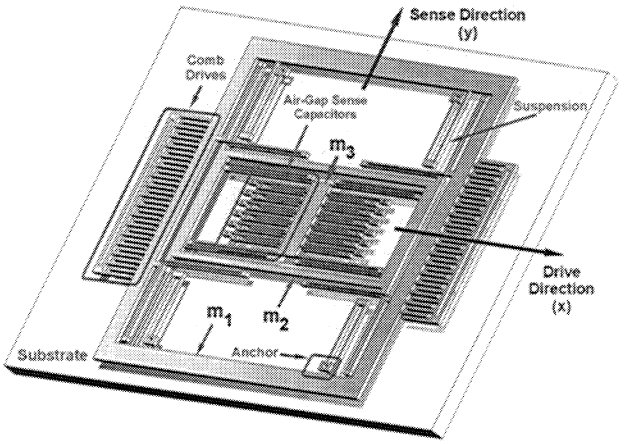

Figure 1: Conceptual schematic of the micromachined 4-DOF gyroscope with decoupled oscillation modes.

$$m\ddot{x} + c_x\dot{x} + (k_x - m{\Omega_z}^2)x = F_d + m\dot{\Omega}_z y + 2m\Omega_z\dot{y}$$
$$m\ddot{y} + c_y\dot{y} + (k_y - m{\Omega_z}^2)y = -m\dot{\Omega}_z x - 2m\Omega_z\dot{x}.$$

where m is the proof mass, F_d is the drive direction excitation force, and Ω_z is the input angular rate. The two final terms $2m\Omega_z\dot{y}$, and $2m\Omega_z\dot{x}$ are the rotation-induced Coriolis forces, causing dynamic coupling between the oscillation axes proportional to the angular rate input. The 2-DOF dynamical system will have the two distinct resonance frequencies $\omega_x = \sqrt{k_x/m}$, and $\omega_y = \sqrt{k_y/m}$ in the drive and sense modes, respectively.

The proof mass is generally sustained in resonance in the drive direction. To achieve high sensitivity, the drive and the sense resonant frequencies are typically designed and tuned to match, i.e. $\omega_x = \omega_y$, and the device is controlled to operate at or near the peak of the response curve [4]. To enhance the sensitivity further, the device is packaged in high vacuum, minimizing energy dissipation due to viscous effects of air surrounding the mechanical structure. However, when the resonance frequencies are mismatched ($\omega_x \neq \omega_y$), the frequency response of the 2-DOF system has two resonant peaks (Figure 2), one at ω_x, and another at ω_y. However, fabrication imperfections affect both the ge-

ometry and the material properties of MEMS devices [3], while variations in the temperature of the structure perturb the dynamical system parameters due to the temperature dependent material properties and thermally induced localized stresses. The mode-matching requirement renders the system response very sensitive to variations in system parameters due to fabrication imperfections and fluctuations in operating conditions, which shift the drive or sense resonant frequencies.

Extensive research has been focused on design of symmetric suspensions and resonator systems for mode-matching and minimizing temperature dependence [8], [9]. However, especially for lightly-damped devices, the requirement for mode-matching is well beyond fabrication tolerances; and none of the symmetric designs can provide the required degree of mode-matching without feedback control [2]. Furthermore, the mechanical interference between the modes, and thus the operation instability and drift, are proportional to the degree of mode-matching. Various devices have been proposed employing independent flexures for driving and sensing mode oscillations to suppress coupled oscillation and the resulting zero-rate drift [6]–[8].

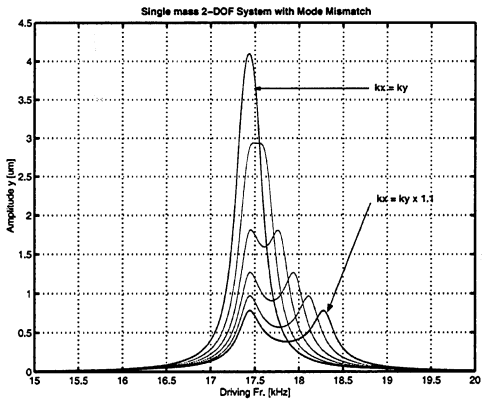

Figure 2: The response of the overall 2-DOF system, which diminishes with increasing drive and sense resonance frequency mismatch.

The 4-DOF gyroscope design concept proposed in this paper (Figure 1) eliminates the limitations due to mode-matching requirement, damping sensitivity and drift due to mechanical interference by utilizing mechanically decoupled 2-DOF non-resonant drive and sense oscillators incorporating three proof masses. 4-DOF MEMS gyroscopes composed of two interconnected proof masses have been reported to achieve improved robustness [5]; however, the drive and sense oscillators can not be mechanically decoupled, and the dynamical response characteristics of the oscillators can not be set independently in these approaches.

2 THE 4-DOF GYROSCOPE STRUCTURE

The 4-DOF micromachined gyroscope system utilizes dynamical amplification in the decoupled 2-DOF drive and sense oscillators to achieve large oscillation amplitudes without resonance. The overall 4-DOF dynamical system, namely 2-DOF in drive and 2-DOF in sense directions, is composed of three interconnected proof masses (Figure 1). The first mass m_1, which is the only mass excited in the drive direction, is constrained in the sense direction, and is free to oscillate only in the drive direction. The second mass m_2 and the third mass m_3 are fixed with respect to each other in the drive direction, thus move as one combined mass in the drive direction. However, m_2 and m_3 are free to oscillate independently in the sense direction, forming the 2-DOF sense-direction oscillator. The first mass m_1 and the combination of the second and third masses $(m_2 + m_3)$ form the 2-DOF drive-direction oscillator, where m_1 is the driven mass (Figure 3).

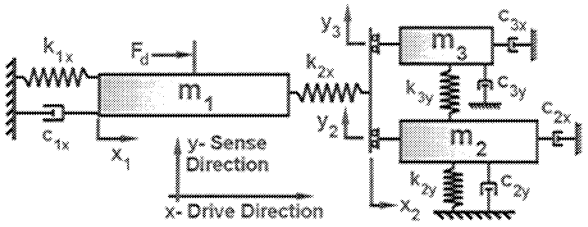

Figure 3: Lumped mass-spring-damper model of the overall 4-DOF gyroscope dynamical system.

In order to minimize instability due to dynamical coupling between the drive and sense modes, the drive and sense direction oscillators are mechanically decoupled. The driven mass m_1 oscillates only in the drive direction, and possible anisoelasticities due to fabrication imperfections are suppressed by the suspension infinitely rigid in the sense direction. The second mass m_2 oscillates in both drive and sense directions, and generates the rotation-induced Coriolis force that excites the 2-DOF sense-direction oscillator. The sense direction response of the third mass m_3, which comprises the vibration absorber of the 2-DOF sense-direction oscillator, is detected for rate measurement. Since the springs that couple the sense element m_3 to m_2 deform only for relative sense direction oscillations, instability due to mechanical coupling of drive and sense directions is minimized, significantly enhancing gyroscopic performance due to reduced drift.

2.1 Suspension Design

The suspension that connects m_1 to the substrate via anchors is comprised of four double-folded flexures (Figure 4), where each beam of length L_{1x} in the folded

flexures can be modeled as a fixed-guided beam deforming in the orthogonal direction to the axis of the beam, leading to an overall stiffness of

$$k_{1x} = \frac{4}{2}\left(\frac{1}{2}\frac{3EI}{\frac{L_{1x}}{2}^3}\right) = \frac{2Etw^3}{{L_{1x}}^3}$$

where E is the Young's Modulus, I is the second moment of inertia of the beam cross-section, t is the beam thickness, and w is the beam width.

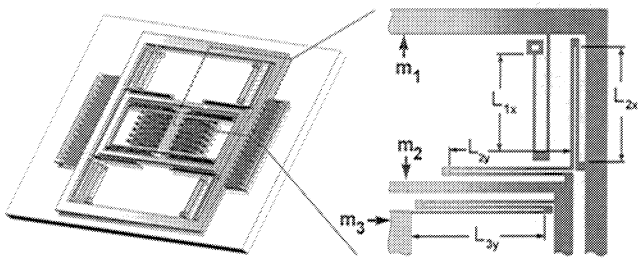

Figure 4: The suspension system configuration that forms the mechanically decoupled 2-DOF drive and sense direction oscillators with the three proof masses.

The second mass m_2 is connected to m_1 by four flexures composed of two double-folded beams of length L_{2x} and L_{2y} that deform independently in the drive and sense directions. The suspension connecting the third mass m_3 to m_2 is made up of four three-folded flexures with a length of L_{3y} fixing m_3 with respect to m_2 in the drive-direction. Since these flexures are stiff in the drive-direction zero-rate drift due to mechanical interference in the sensing element m_3 is eliminated. These beams can also be modeled similarly, yielding the stiffness values of

$$k_{2x} = \frac{2Etw^3}{{L_{2x}}^3},\ k_{2y} = \frac{2Etw^3}{{L_{2y}}^3},\ k_{3y} = \frac{4}{3}\frac{Etw^3}{{L_{3y}}^3}$$

3 DYNAMICS OF THE GYROSCOPE

The dynamics of the idealized model for the 4-DOF gyroscope system is best understood in the non-inertial coordinate frame associated with the gyroscope. The 4-DOF system consists of three interconnected proof masses where each mass can be assumed to be a rigid body with a position vector $\vec{r}$ attached to a rotating reference frame B, resulting in an absolute acceleration in the inertial frame A:

$$\vec{a_A} = \vec{a_B} + \vec{\Omega} \times \vec{r_B} + \vec{\Omega} \times (\vec{\Omega} \times \vec{r_B}) + 2\vec{\Omega} \times \vec{v_B}$$

where the subscript A denotes "relative to inertial frame A", B denotes "relative to rotating gyroscope frame B", $\vec{v_B}$ and $\vec{a_B}$ are the velocity and acceleration vectors with respect to the reference frame, respectively, and $\vec{\Omega}$ is the angular velocity of the gyroscope frame. The term $2\vec{\Omega} \times \vec{v_B}$ is the Coriolis acceleration, and excites the system in the sense direction. Similarly, the equations of motion for the three proof masses observed in the non-inertial rotating frame can be expressed in the inertial frame as:

$$m_1\vec{a_1} = \vec{F_1} + \vec{F_d} - 2m_1\vec{\Omega} \times \vec{v_1} - m_1\vec{\Omega} \times (\vec{\Omega} \times \vec{r_1}) - m_1\dot{\vec{\Omega}} \times \vec{r_1}$$
$$m_2\vec{a_2} = \vec{F_2} - 2m_2\vec{\Omega} \times \vec{v_2} - m_2\vec{\Omega} \times (\vec{\Omega} \times \vec{r_2}) - m_2\dot{\vec{\Omega}} \times \vec{r_2}$$
$$m_3\vec{a_3} = \vec{F_3} - 2m_3\vec{\Omega} \times \vec{v_3} - m_3\vec{\Omega} \times (\vec{\Omega} \times \vec{r_3}) - m_3\dot{\vec{\Omega}} \times \vec{r_3}$$

where $\vec{F_1}$ is the net external force applied on m_1 including elastic and damping forces from the substrate and elastic interaction force from m_2; $\vec{F_2}$ is the net external force applied on m_2 including the damping force from the substrate and elastic interaction force from m_1 and m_3; $\vec{F_3}$ is the net external force applied on m_3 including the damping force from the substrate and the elastic interaction force from m_2; and $\vec{F_d}$ is the driving force applied on m_1. In the gyroscope frame, $\vec{r_1}$, $\vec{r_2}$, and $\vec{r_3}$ are the position vectors; and $\vec{v_1}$, $\vec{v_2}$, and $\vec{v_3}$ are the velocity vectors of m_1, m_2 and m_3, respectively. Since the first mass is fixed in the sense direction, i.e. $y_1(t) = 0$, and m_2 and m_3 move together in the drive direction, i.e. $x_2(t) = x_3(t)$; the 4-DOF equations of motion (along the x-axis and y-axis) of the three masses subject to an angular rate of Ω_z about the axis normal to the plane of motion (z-axis) become:

$$m_1\ddot{x_1} + c_{1x}\dot{x_1} + k_{1x}x_1 = k_{2x}(x_2 - x_1) + m_1\Omega_z^2 x_1 + F_d(t)$$

$$(m_2 + m_3)\ddot{x_2} + (c_{2x} + c_{3x})\dot{x_2} + k_{2x}(x_2 - x_1) = (m_2 + m_3)\Omega_z^2 x_2 + 2m_2\Omega_z\dot{y_2} + 2m_3\Omega_z\dot{y_3} + m_2\dot{\Omega}_z y_2 + m_3\dot{\Omega}_z y_3$$

$$m_2\ddot{y_2} + c_{2y}\dot{y_2} + k_{2y}y_2 =$$
$$k_{3y}(y_3 - y_2) + m_2\Omega_z^2 y_2 - 2m_2\Omega_z\dot{x_2} - m_2\dot{\Omega}_z x_2$$

$$m_3\ddot{y_3} + c_{3y}\dot{y_3} + k_{3y}(y_3 - y_2) =$$
$$m_3\Omega_z^2 y_3 - 2m_3\Omega_z\dot{x_3} - m_3\dot{\Omega}_z x_3.$$

where $F_d(t)$ is the driving electrostatic force applied to the active mass at the driving frequency ω_d, and Ω_z is the angular velocity applied to the gyroscope about the z-axis. It should be noticed that the terms $2m_2\Omega_z\dot{x_2}$ and $2m_3\Omega_z\dot{x_3}$ are the Coriolis forces that excite the system in the sense direction, and the Coriolis response of m_3 in the sense-direction (y_3) is detected for angular rate measurement.

The dynamical system parameters used in the simulations in the next section are: $m_1 = 3.9 \times 10^{-10}$kg, $m_2 = 2.73 \times 10^{-10}$kg, $m_3 = 2.48 \times 10^{-11}$kg, $k_{1x} = 2.01$N/m, $k_{2x} = 1.55$N/m, $k_{2y} = 1.74$N/m, and $k_{3y} = 0.141$N/m, which were obtained through Finite Element Analysis in the MSC Nastran/Patran software package.

4 THE CORIOLIS RESPONSE

The frequency responses of the 2-DOF drive direction oscillator and the 2-DOF sense direction oscillator have two resonant peaks and a flat region between the peaks. The device is nominally operated in the flat regions of the drive and sense direction oscillators, where the response amplitudes of the oscillators are insensitive to parameter variations. In order to operate both of the

of the drive and sense direction oscillators in their flat-region frequency bands, the flat regions of the oscillators have to be designed to overlap (Figure 5a), by matching the drive and sense direction anti-resonance frequencies. Thus, the requirement $\sqrt{\frac{k_{3y}}{m_3}} = \sqrt{\frac{k_{2x}}{(m_2+m_3)}}$ determines the optimal system parameters. However, in contrast to the conventional gyroscopes, the flat regions with significantly wider bandwidths can be overlapped without feedback control with sufficient precision despite fabrication imperfections and operation condition variations.

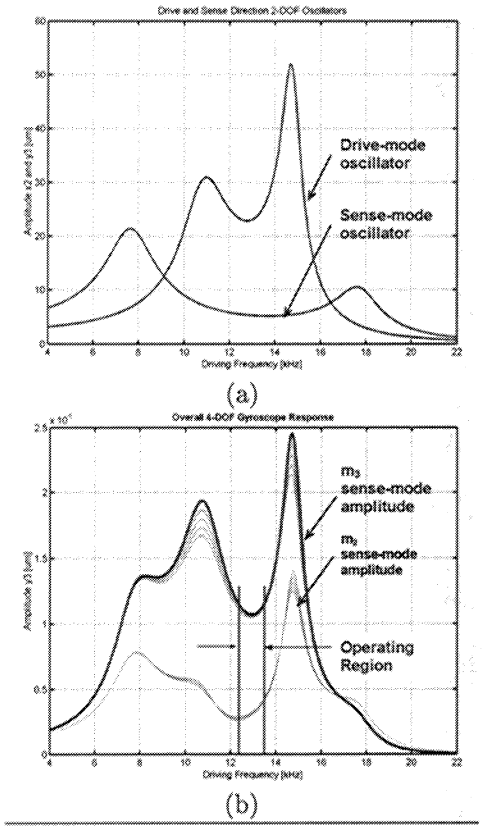

Figure 5: (a) The frequency responses of the 2-DOF drive and sense-mode oscillators, with the overlapped flat regions. (b) The response of the overall 4-DOF gyroscope system. The oscillation amplitude is insensitive to parameter variations and damping fluctuations in the flat operating region.

The response of the combined 4-DOF dynamical system to the rotation-induced Coriolis force will have a flat region in the frequency band coinciding to the flat regions of the independent drive and sense-mode oscillators (Figure 5b). When the device is operated in this flat region, the oscillation amplitudes in both drive and sense directions are relatively insensitive to variations in system parameters and damping. Thus, by utilizing dynamical amplification in the 2-DOF oscillators instead of resonance, increased bandwidth and reduced sensitivity to structural and thermal parameter fluctuations and damping changes are achieved.

5 CONCLUSION

In this paper, a novel 4-DOF non-resonant micromachined gyroscope design concept is reported, which eliminates the mode-matching requirement, and minimizes instability and zero-rate drift due to mechanical coupling between the drive and sense modes. The proposed approach is based on utilizing dynamical amplification in mechanically decoupled 2-DOF drive-mode oscillator and 2-DOF sense-mode oscillator formed by three interconnected proof masses. Attaining large oscillation amplitudes without resonance resulting in increased bandwidth and reduced sensitivity to structural and thermal parameter fluctuations and damping changes; while mechanically decoupling the drive direction oscillations from the sense direction oscillations leads to improved robustness and long-term stability over the operating time of the device.

6 ACKNOWLEDGEMENTS

This work is supported in part by the National Science Foundation Grant CMS-0223050.

REFERENCES

[1] N. Yazdi, F. Ayazi, and K. Najafi. Micromachined Inertial Sensors. *Proceedings of IEEE, Vol. 86, No. 8*, August 1998, pp. 1640-1658.

[2] S. Park and R. Horowitz. Adaptive Control for Z-Axis MEMS Gyroscopes. *American Control Conference, Arlington, VA*, June 2001.

[3] A. Shkel, R.T. Howe, and R. Horowitz. Modeling and Simulation of Micromachined Gyroscopes in the Presence of Imperfections. *International Conference on Modeling and Simulation of Microsystems*, Puerto Rico, 1999, pp. 605-608.

[4] W.A. Clark. Micromachined Vibratory Rate Gyroscope. *Ph.D. Thesis, BSAC, U.C. Berkeley*, 1994.

[5] C. Acar, and A. Shkel. Four Degrees-of-Freedom Micromachined Gyroscopes. *Journal of Modeling and Simulation of Microsystems, Vol. 2, No. 1*, pp. 71-82, 2001.

[6] J.A. Geen. A Path to Low Cost Gyroscopy. *Solid-State Sensor and Actuator Workshop*, Hilton-Head, SJ, 1998, pp. 51-54.

[7] W. Geiger, W.U. Butt, A. Gaisser, J. Fretch, M. Braxmaier, T. Link, A. Kohne. Decoupled Microgyros and the Design Principle DAVED. *IEEE Sensors Journal*, 2001, pp. 170-173.

[8] S.E. Alper, and T. Akin. Symmetric Micromachined Gyroscope with Decoupled Oscillation Modes. *Sensors and Actuators A*, Vol. 97, 2002, pp. 347-358.

[9] Y.S. Hong, J.H. Lee, and S.H. Kim. A Laterally Driven Symmetric Micro-Resonator for Gyroscopic Applications. *Journal of Micromechanics and Microengineering*, Vol. 10, 2000, pp. 452-458.